THz wave emission from Cu_2O/Cu interface under femtosecond laser irradiation

Yuen-ting Rachel Chau[1], Hsin-hui Huang[2], Mai Thanh Nguyen[1], Koji Hatanaka[2,3,4]* and Tetsu Yonezawa[1,5]*

[1]*Division of Materials Science and Engineering, Faculty of Engineering, Hokkaido University, Kita 13 Nishi 8, Kita-ku, Sapporo, Hokkaido 060-8628, Japan*

[2]*Research Center for Applied Sciences, Academia Sinica, Taipei 11529, Taiwan*

[3]*College of Engineering, Chang Gung University, Taoyuan 33302, Taiwan*

[4]*Department of Materials Science and Engineering, National Dong-Hwa University, Hualien 97401, Taiwan*

[5]*Institute for the Promotion of Business-Regional Collaboration, Hokkaido University, Hokkaido 001-0021, Japan*

E-mail: kojihtnk@gate.sinica.edu.tw, tetsu@eng.hokudai.ac.jp

Cu or Cu/Au (80nm-thick Cu, 50nm-thick Au) sputtered on Si were kept at 25 °C for a week or annealed at temperature from 80 to 300 °C, then tested for THz emission under femtosecond laser irradiation (35 fs-800nm). THz radiation was detected from samples annealed from 80 to 170 °C, which had Cu_2O/Cu interface as the THz source. Cu/Au/Si annealed at 80 °C emitted the highest THz radiation because of high laser absorption by the porous Cu_2O layer formed at low temperature and the Au film reflected THz radiation and/or increased the laser absorption by Fabry–Pérot effect.

Studies of THz radiation are impelled by applications such as non-destructive examination[1-3], biological molecules detection[4,5] and broadband communication.[6,7] It is known that ZnTe and GaAs are promised THz sources under ultrafast pulse laser irradiation.[8-10] The laser pulses accelerate charge carriers at the air/semiconductor interface, where the depletion field (also known as Schottky field) exists, and develop a transient current as the source of THz radiation.[11,12]

Cuprous oxide (Cu_2O) is also an attractive THz source because it is low-cost.[13-17] Several reports found the THz wave emission enhancement from Cu_2O, which was formed via oxidative annealing of Cu layer, on Au/Si substrate.[14-17] For example, Ramakrishnan *et al.* demonstrated the THz wave emission intensity increased with the thickness of Cu_2O layer and a 420nm-thick Cu_2O layer had the highest THz wave emission was observed in their study. Such enhancement of THz radiation was due to more void spaces existed in a thicker layer, promoting laser absorption. They also found that Cu_2O films with thickness less than 100 nm, annealed at temperature of 250 °C for 3 h emitted almost zero THz wave.[17] It is noted that the temperature for oxidizing a Cu film in air is an important factor since high temperature promotes the oxidation rate of Cu and influences the thickness, grain size and porosity of the oxide layer. We found different annealing temperatures (110 °C,[14,15] 220 °C,[16] 250 °C[17]) were used in the literatures for oxidizing the Cu film to Cu_2O as THz source, but there is no report regarding the effect of the annealing temperature of a Cu film to the THz wave emission intensity.

Here, we report the THz wave emission from annealed Cu film with respect to the annealing temperature on Si or Au/Si substrates. The Cu/Si or Cu/Au/Si structures are prepared by sputtering metal films on Si substrate. Both structures have the highest THz wave emission intensity after annealing at temperature of 80 °C for 2.5 h. THz wave emission decreased from Cu/Si or Cu/Au/Si structures by increasing the annealing temperature from 80 to 300 °C. It is suggested that the THz wave emission from annealed Cu film is owing to Cu_2O/Cu interface based on the findings of material characterization.

Non-doped <100>-oriented Si wafers (Global Top Chemical, Japan) with size of 1 cm^2 were the substrate. The wafers were washed with acetone by ultrasonic bath and rinsed with distilled water. They were put into 8% HF solution for 20 min to etch away the SiO_2 on the surface followed with UV-ozone cleaning. Sputtering was used for metal film deposition.

Sputtering pressure and current were 2 Pa and 30 mA, respectively. To prepare single Cu structures, Cu (99.99% in purity, 50 mm in diameter, Nilaco, Japan) target was sputtered for 25.5 min. To prepare Cu/Au structures, Au (99.99% in purity, 50 mm in diameter, Tanaka Precious Metals, Japan) was sputtered for 6.5 min followed with sputtering Cu for 25.5 min. Both structures were kept at ambient (25 °C) for a week or annealed in a maffle furnace for 2.5 h at 80, 110, 140, 170, 200, 250 and 300 °C, respectively. X-ray diffraction (XRD, Rigaku MiniFlex II, Cu Ka radiation, λ= 0.15418 nm , scanning range = 30 to 75°) was conducted for Cu films before and after annealing. Transmission electron microscope (TEM, JEOL FX-2000, 200 kV) observation was performed to measure film thickness after sample preparation with focus ion beam (FIB).

Laser irradiation experiments for THz time-domain spectroscopy (TDS) were carried out in a usual manner. Femtosecond laser pulses (35fs/transform-limited, 800nm, 1 kHz, Mantis/Legend Elite HE USP, Coherent) were irradiated without focusing to the sample surface, which is held on a conventional mirror holder, with the incident angle of 45°. The incident laser intensity was fixed at 0.14 mJ/pulse and the beam diameter was 8 mm. THz wave emission toward the reflection direction was transferred to a setup for electro-optic sampling with a <110>-oriented ZnTe single crystal (1-mm thick, Nippon Mining & Metals, Co. Ltd.). Measurements with lock-in detection were carried out with a chopper (3502, New Focus) and a lock-in amplifier (SR830, Stanford Research System), the effective laser repetition is 0.5 kHz. No apparent sample damages were recognizable after the laser irradiation experiments. TDS signals were obtained and THz wave emission spectra were calculated by discrete Fourier-transform (DFT) of the TDS signals. The optical path length from the sample surface to the ZnTe crystal is 70 cm. All the laser irradiation experiments were carried out in atmospheric pressure in air (23 °C with 40-50 % humidity). Sharp absorption lines observed in DFT spectra, at 0.55 THz for instance, are due to THz absorption by water components[18] in atmosphere.

Fig. 1 shows the XRD patterns (range = 34 to 46°) of as-sputtered and annealed Cu/Si. The patterns were normalized by taking the intensity of Si (400) peak at 69° from the Si substrate as the highest point and the smallest value from the data as the lowest point. The as-sputtered Cu film had a broad peak located at 43.3° for Cu (111) plane. The broad peak indicated that the crystalline size was small. The peak located at 36.4° in the pattern of

sample annealed at 80 °C represented Cu_2O (111) plane. The intensity of Cu_2O (111) peak was increased relatively to that of Cu (111) peak by increasing temperature from 80 to 140 °C. The intensity of the strongest peak of Cu and its oxides was used to roughly estimate the relative content of Cu_2O (wt.%) in the film.[19] Table I shows the calculated Cu_2O (wt.%) from the films annealed at 80, 110 and 140 °C. It should be noted that the as-deposited film contained lots of small grains which contributed low and broad signals to the Cu and Cu_2O peaks in XRD pattern of as-sputtered and annealed film, respectively. Thus, the estimated Cu_2O content listed in Table I was an approximation value. The sample annealed at 170 °C showed significant peaks of Cu_2O (111) and (200) planes. Raising the annealing temperature to 250 °C resulted in both Cu_2O and CuO phases and only CuO phase existed at 300 °C.[20,21] The characteristic peaks became less broaden as the annealing temperature increased due to the crystal growth. On the other hand, the Cu film kept under ambient for 1 week had the characteristic peak of Cu_2O (111) plane due to the oxidation behavior of Cu when it contacted with oxygen molecules in the air.[22]

The cross-sectional image of Cu/Au double-layered structure on Si substrate annealed at 110 °C was captured by TEM (Fig. 2(a)). The Au and Cu layers had average thickness of 54 and 80 nm, respectively. A selected area electron diffraction (SAED) pattern (Fig. 2(b)) was taken at the uppermost surface of Cu layer (red circle #1 in Fig. 2(a)). The diffraction rings were indexed as (111), (200), (220) and (311) for Cu_2O (JCPDS No. 005-0667). The SAED pattern was taken at the area having both Cu and Au layers (red circle #2 in Fig. 2(a)) and the diffraction rings of Cu (111) (JCPDS No. 004-0836) and Au (111), (200), (220) and (311) (JCPDS No. 041-0254) were observed (Fig. 2(c)). The SAED results suggested that the structure actually had Cu_2O/Cu/Au layers. Although the XRD pattern suggested the Cu film annealed at 110 °C composed with Cu and Cu_2O, the diffraction pattern of Cu was not observed at the surface of Cu layer in Fig. 2. It was because the oxidation started at the surface of Cu film while the selected area only had Cu_2O and XRD pattern was accounted for the total thickness of the film.

Fig. 3 shows the TDS signals and DFT spectra measured from Cu/Si and Cu/Au/Si structures treated at different conditions. Cu/Si annealed at 80 °C had the highest THz wave emission. The intensity of emission was then decreased at temperature of 110 and 140 °C and became even lower at temperature $\geq$ 170 °C. These suggest the THz wave emission

was attributed to the Cu_2O/Cu interface, where the depletion region existed, in the samples annealed at 80, 110, 140 and 170 °C. The Cu_2O layer with porous structure possibly emits higher THz wave was reported because the cavities in the film can concentrate the incident laser pump, allowing more photoexcitation occurs.[17] The Cu_2O layer was less porous due to the grain growth as the temperature was increased. Therefore, when the temperature was increased from 80 to 170 °C, the decrease in the THz wave emission from the Cu_2O/Cu interface might owing to the denser structure formed in the Cu_2O layer. Furthermore, Cu film annealed at 200, 250 and 300 °C consisted of an oxide film without Cu_2O/Cu interface, consequently resulted in the weak emission. Besides, the THz wave emission intensity might related to the content of Cu_2O in the Cu layer, since Cu_2O content from Cu/Si kept in ambient for 1 week (48.1%) was close to the that of Cu/Si annealed at 110 °C for 2.5 h (49.0%) and they had similar THz wave emission intensity.

For the Cu/Au/Si structures, enhancement of THz emission from Cu_2O/Au structure was reported elsewhere.[14-17] So that, Cu/Au/Si annealed at 200 °C was expected to have the highest THz wave emission since it consisted of only Cu_2O phase according to the XRD pattern. However, the results showed that Cu/Au/Si structures annealed at 80 °C had the highest THz wave emission. Fig. 4 summarizes the THz wave emission intensity from annealed Cu/Si (blue triangles) and Cu/Au/Si (red circles) structures against the annealing temperature. When annealing temperature was below 200 °C, annealed Cu/Au/Si structures had higher THz wave emission than Cu/Si structures. There were two possible reasons: (1) THz wave emitted from the Cu_2O/Cu interface propagated in all directions and the Au layer reflected the THz wave, therefore higher THz wave intensity was detected from Cu/Au/Si structures,[17] and (2) THz wave emission was enhanced due to Fabry–Pérot interference occurred in Au layer, which increased absorption of incident laser.[17,23] The reflectance spectra (Fig. S2) showed both the Si substrate and the Cu/Au/Si samples absorbed light (> 98%) near 800 nm. The absorption of the Cu/Au double layers was enhanced significantly compared with a Cu layer when they were deposited on a transparent glass slide (Fig. S3). Fabry–Pérot interference was possibly arose but it cannot be deduced that the incident light was totally absorbed by the Au layer or the substrate when using Si wafer. Furthermore, less THz wave emission was detected from both annealed Cu/Si and Cu/Au/Si structures when the annealing temperature was at $\geq$ 200 °C. This is attributed to the lack of depletion region

in those samples, which can be explained by the work function of materials. Cu_2O has work function of 4.84 eV[24] which is smaller than Au (5.1 eV[25]). An ohmic contact was formed in Cu_2O/Au[26] and CuO/Au.[27,28] Thus, almost zero emission from samples annealed at $\geq$ 200 °C. Diffusion was also occurred in between Cu and Au layers during annealing.[15,16,29] When the Cu atoms diffused to Au layer, the work function of Au layer decreased to be smaller than that of Cu_2O and formed a depletion region.[16] This induced the THz wave emission intensity from Cu/Au/Si structure was higher than that of Cu/Si structure at annealing temperature of 170 °C. Nonetheless, both Cu/Au/Si structures that were kept in ambient for 1 week and annealed at 110 °C did not show significant enhancement in THz wave emission. The reason of the insignificant enhancement remains elusive. Moreover, other pieces of Cu/Si prepared at 200, 250 and 300 °C were tested and large variation of THz wave emission intensity was discovered (inset in Fig. 4). The THz wave emission intensity from single-layered samples was higher than double-layered ones can be considered as experimental errors.

Our results are different from Ramakrishnan *et al.*,[17] they found the Cu_2O/Au structure (by annealing Cu/Au structure at 250 °C for 3 h) had almost zero THz wave emission when the thickness of Cu_2O layer was less than 100 nm. We herewith found that the THz wave emission was enhanced by annealing samples at lower temperature (80 °C), whereas the Cu_2O film thickness was in the range of less than 100 nm. The main differences are attributed for the smaller the grain size and higher porosity of the Cu_2O layer formed by annealing at lower temperatures in our case, while they annealed the Cu films at 250 °C to form Cu_2O on Au and found the Cu_2O films with thickness less than 100 nm had almost zero THz emission in their case.[17] At annealing temperature of 250 °C and Cu_2O film thickness less than 100 nm, our samples also emitted almost zero THz radiation (Fig. 3(h)). It is noteworthy that thickness of semiconductor layer determines the THz wave emission intensity because a thicker film can enhance the laser absorption and expands the depletion region of semiconductor.[17,30]

Likewise, the double-layered structure was inverted, i.e., Au/Cu/Si by depositing the Au layer on top of an annealed Cu layer. It is because the uppermost Au layer can protect the Cu layer from further oxidation, which causes the reduction in THz wave emission. Figure S1. (see supplementary data) shows the THz wave emission intensity from Cu/Au/Si

and Au/Cu/Si structures annealed at 110 °C for comparison. The THz wave emission intensity from Au/Cu/Si structure was weaker than that of Cu/Au/Si because of the incident laser power loss in Au layer.[14] Hence, Au film is not suitable for preventing further oxidation of Cu for designing a sustainable THz source.

In summary, the THz wave emission was observed from Cu_2O/Cu interface under femtosecond laser excitation. Although it was reported that less than 100nm-thick Cu_2O layer annealed at 250 °C emitted almost no THz, we found that Cu_2O/Cu interface formed by annealing 80nm-thick Cu layer at temperature of 80 to 170 °C can enhance the THz wave emission. Especially at 80 °C, the Cu/Si gave the highest THz wave emission intensity. It was possibly due to the highly porous structure of Cu_2O layer formed at low temperature, which can promote the laser absorption. The THz wave emission was decreased at annealing temperature of $\geq$ 200 °C. It was because Cu layer did not have Cu_2O/Cu interface and/or lack of porous structure from grain growth at that high annealing temperature. The Cu/Au/Si structures also had similar THz wave emission trend with respect to the annealing temperatures. From that, Cu/Au/Si annealed at 80 °C showed increased in THz wave emission by 41.4% compared with Cu/Si annealed at same temperature. The Cu/Au/Si structures annealed at $\geq$ 200 °C also had almost zero THz wave emission because of the formation of ohmic contact at Cu_2O/Au and CuO/Au interfaces. Au/Cu/Si structure was also prepared and annealed at 110 °C. The inverted structure had very low THz wave emission compared with Cu/Au/Si because of the dissipation of laser energy at the Au film.

Acknowledgments

Y.R.C. thank for Prof. T. Shibayama and Ms. M. Kondo (Hokkaido Univ.) for the FIB support. K. H. is grateful for the supports by the Ministry of Science and Technology (MOST) of Taiwan (107-2112-M-001-014-MY3), the Cooperative Research Program of "Network Joint Research Center for Materials and Devices", Nanotechnology Platform (Hokkaido University), and the Collaborative Research Projects of Laboratory for Materials and Structures, Institute of Innovative Research (Tokyo Institute of Technology). T. Y. thank for the financial support by Grant-in-Aid for Scientific Research for Fostering Joint International Research (B) (18KK0159), the Cooperative Research Program of "Network Joint Research Center for Materials and Devices". M.T. thank for the financial support from Grant for Basic Science Research Project from Sumitomo foundation.

References

1) J.B. Jackson, M. Mourou, J.F. Whitaker, I.N. Duling, S.L. Williamson, M. Menu, and G.A. Mourou, Opt. Commun., **281**, 527 (2008).
2) C.D. Stoik, M.J. Bohn and J.L. Blackshire, Opt. Express, **16**, 17039 (2008).
3) A.J.L. Adam, P.C.M. Planken, S. Meloni and J. Dik, Opt. Express, **17**, 3407 (2009).
4) D. Lee, J. Kang, J. Lee, H. Kim, C. Kim, J. Hun Kim, T. Lee, J. Son, Q. Park, and M. Seo, Sci. Rep., **5**, 15459 (2015).
5) T.R. Globus, D.L. Woolard, T. Khromova, T.W. Crowe, M. Bykhovskaia, B.L. Gelmont, J. Hesler and A.C. Samuels, J. Biol. Phys., **29**, 89 (2003).
6) R. Piesiewicz, T. Kleine-Ostmann, N. Krumbholz, D. Mittleman, M. Koch, J. Schoebel and T. Kurner, IEEE Antennas Propag. Mag., **49**, 24 (2007).
7) R. Heidemann, T. Pfeiffer and D. Jäger, Electron. Lett., **19**, 316 (1983).
8) G. Mourou, C.V. Stancampiano, A. Antonetti, and A. Orszag, Appl. Phys. Lett., **39**, 295 (1981).
9) A. Rice, Y. Jin, X.F. Ma, X.-C. Zhang, D. Bliss, J. Larkin and M. Alexander, Appl. Phys. Lett., **64**, 1324 (1994).
10) G.L. Dakovski, B.Kubera and J. Shan, J. Opt. Soc. Am. B, **22**, 1667 (2005).
11) X.-C. Zhang, J.T. Darrow, B.B. Hu, D.H. Auston, M.T. Schmidt, P. Tham, and E.S. Yang, Appl. Phys. Lett., **56**, 2228 (1990).
12) S.L. Chuang, S. Schmitt-Rink, B.I. Greene, P.N. Saeta and A.F.J. Levi, Phys. Rev. Lett., **68**, 102 (1992).
13) J. Lopez, A. Cafe, H.A. Husay, L. Lopez, A. Salvador, E. Estacio, and A. Somintac, Proc. of the Samahang Pisika ng Pilipinas, 2016, SPP-2016-2A-06.
14) X. Lu and T. Yonezawa, MWP/APMP 2014, 2014, p. 164.
15) X. Lu, Y. Ishida, T. Mishina, M.T. Nguyen, and T. Yonezawa, Bull. Chem. Soc. Jpn., **88**, 1385 (2015).
16) G.K.P. Ramanandan, A.J.L. Adam, G. Ramakrishnan, P. Petrik, R. Hendrikx and P.C.M. Planken, Appl. Opt., **53**, 1994 (2014).
17) G. Ramakrishnan, G.K.P. Ramanandan, A.J.L. Adam, M. Xu, N. Kumar, R.W.A. Hendrikx, and P.C.M. Planken. Opt. Express, **21**, 16784 (2013).
18) M. V. Exter, C. Fattinger, and D. Grischkowsky, Opt. Lett., **14**, 1128 (1989).
19) L. Hu, Y. Huang, F. Zhang and Q. Chen, Nanoscale, **5**, 4186 (2013).
20) V. Kumar, S. Masudy-Panah, C.C. Tan, T.K.S. Wong, D.Z. Chi, and G.K. Dalapati, IEEE INEC, 2013, p. 443.
21) N. Serin, T. Serin, Ş. Horzum and Y. Çelik, Semicond. Sci. Technol., **20**, 398 (2005).
22) I. Platzman, R. Brener, H. Haick, and R. Tannenbaum, J. Phys. Chem. C, **112**, 1101 (2008).
23) P. Bai, Y.H. Zhang, X.G. Guo, Z.L. Fu, J.C. Cao, and W.Z. Shen, Appl. Phys. Lett., **113**, 241102 (2018).
24) W.Y. Yang and S.W. Rhee, Appl. Phys. Lett., **91**, 232907 (2007).
25) D.E. Eastman, Phys. Rev. B, **2**, 1 (1970).
26) R. Gupta, S.C.K. Misra, B.D. Malhotra, N.N. Beladakere, and S. Chandra, Appl. Phys. Lett., **58**, 51 (1991).

252 27) B. Singh and B.R. Mehta, Thin Solid Films, **569**, 35 (2014).
253 28) A.T. Ping, M. Asif Khan, and I. Adesida, J. Electron. Mater., **25**, 819 (1996).
254 29) H.G. Tompkins and M.R. Pinnel, J. Appl. Phys., **47**, 3804 (1976).
255 30) A.C. Adams and B.R. Pruniaux, J. Electrochem. Soc., **120**, 408 (1973).
256

Figure Captions

Fig. 1. XRD patterns of Cu films at different conditions: (a) as-sputtered, keep in ambient for 1 week, annealed at 80, 110, 140, (b) 170, 200, 250 and 300 °C.

Fig. 2. (a) TEM image of the cross-sectional Cu/Au/Si structure annealed at 110 °C for 2.5 h and (b-c) the corresponding diffraction patterns taken by SAED at selected area #1 and #2.

Fig. 3. THz-TDS measurement of the annealed (a-b) Cu/Si and (c-d) Cu/Au/Si structures and (e-h) the corresponding emission spectra at different annealing conditions.

Fig. 4. Total THz wave emission intensity of annealed Cu/Si and Cu/Au/Si structures against different annealing conditions. Solid lines are the guide for the eye.

290 **Table I.** Estimated amount of Cu_2O (wt.%) in the Cu film annealed at 80, 110 and 140 °C.

291

Condition	Cu_2O (wt.%)
80 °C, 2.5 h	47.0
110 °C, 2.5 h	49.0
140 °C, 2.5 h	52.6

292

293

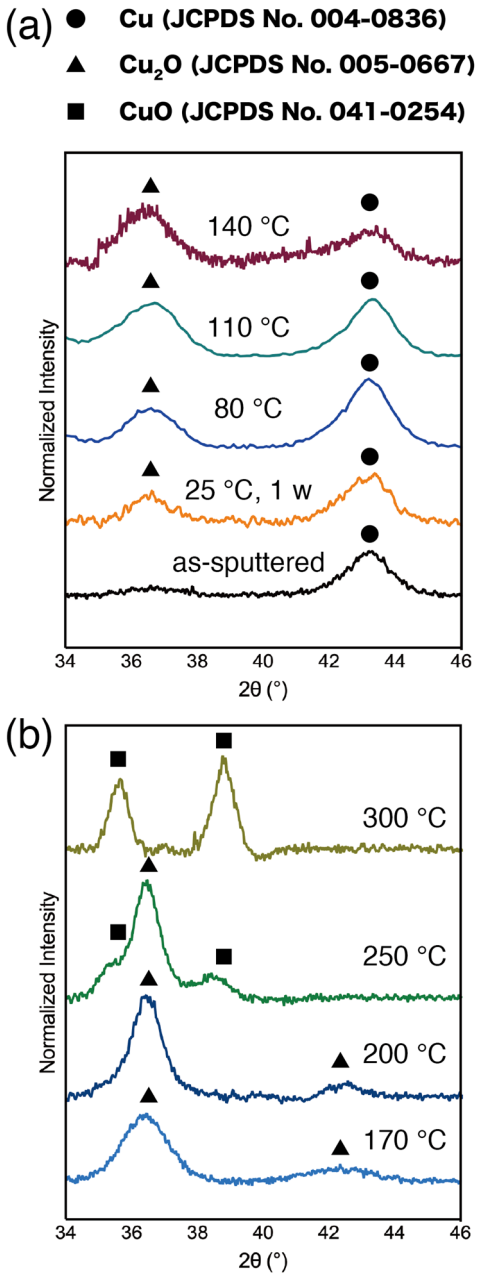

294

295 Fig.1. XRD patterns of Cu films at different conditions: (a) as-sputtered, keep in

296 ambient for 1 week, annealed at 80, 110, 140, (b) 170, 200, 250 and 300 °C.

297

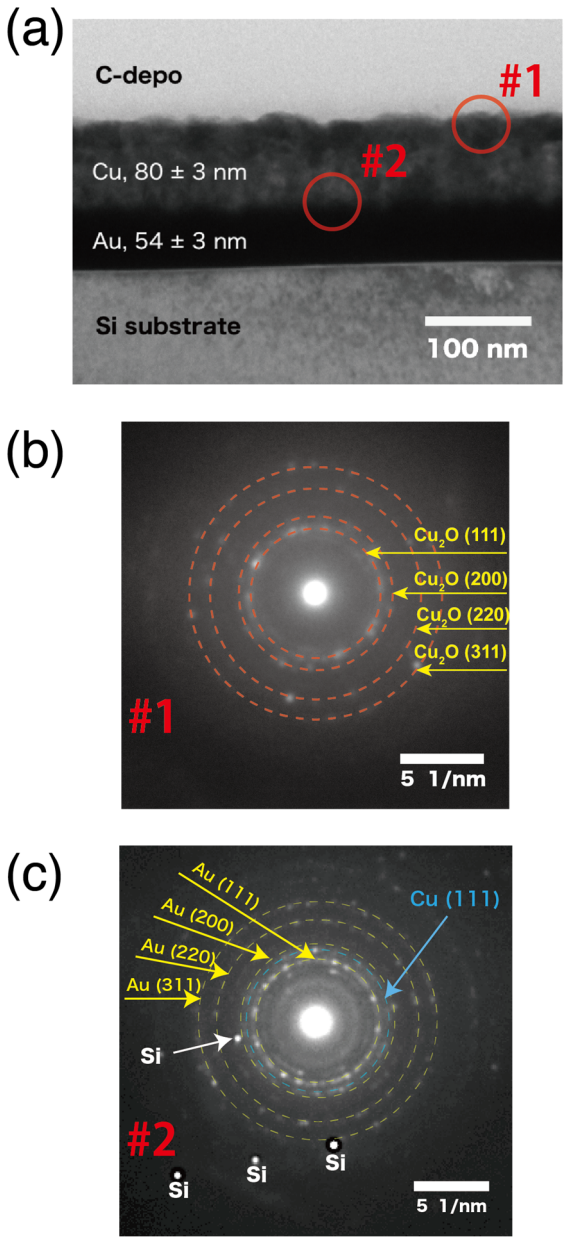

Fig. 2. (a) TEM image of the cross-sectional Cu/Au/Si structure annealed at 110 °C for 2.5 h and (b-c) the corresponding diffraction patterns taken by SAED at selected area #1 and #2.

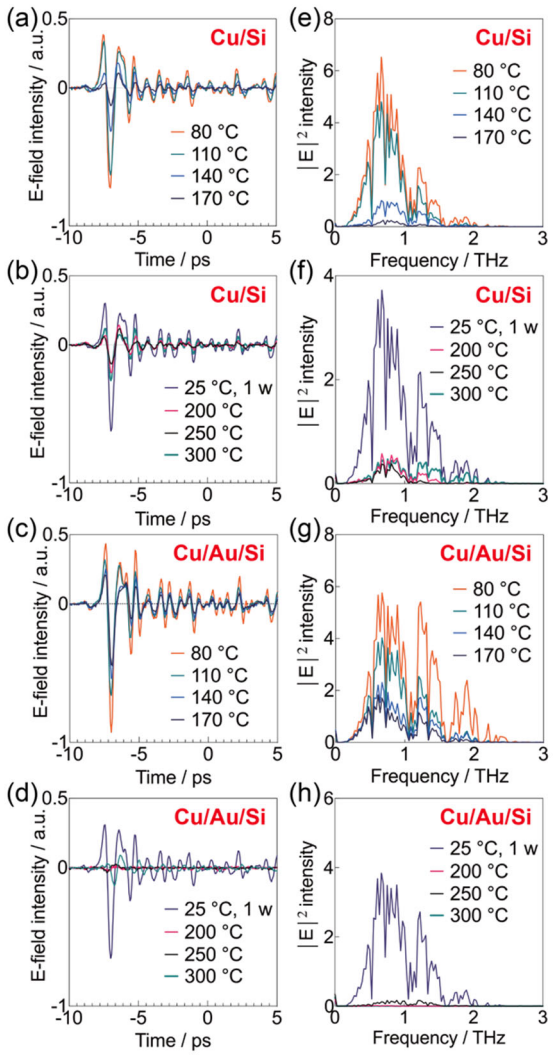

Fig. 3. THz-TDS measurement of the annealed (a-b) Cu/Si and (c-d) Cu/Au/Si structures and (e-h) the corresponding emission spectra at different annealing conditions.

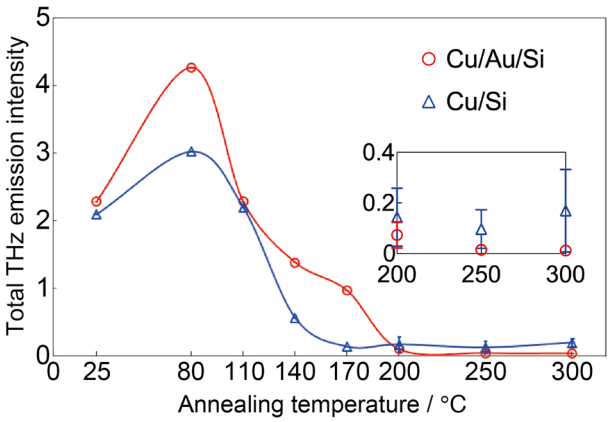

Fig. 4. Total THz wave emission intensity of annealed Cu/Si and Cu/Au/Si structures against different annealing conditions. Solid lines are the guide for the eye.